arXiv:1311.5837v1 [astro-ph.CO] 22 Nov 2013

Non-Statistical Isotropic Gaussian Simulations of the CMB Temperature Field

Suvodip Mukherjee* and Tarun Souradeep†

IUCAA, Post Bag 4, Ganeshkhind, Pune-411007, India

November 25, 2013

Abstract

Although theoretically expected to be Statistically Isotropic (SI), the observed Cosmic Microwave Background (CMB) temperature & polarization field would exhibit SI violation due to various inevitable effects like weak lensing, Doppler boost and practical limitations of observations like non-circular beam, masking etc. However, presence of any SI violation beyond these effects may lead to a discovery of inherent cosmic SI violation in the CMB temperature & polarization field. Recently Planck presented strong evidence of SI violation as a dipolar power asymmetry of the CMB temperature field in two hemispheres. Statistical studies of SI violation effect requires non-SI (nSI) Gaussian realizations of CMB temperature field. The nSI Gaussian temperature field lead to non-zero off-diagonal terms in the Spherical Harmonic (SH) space covariance matrix encoded in the coefficients of the Bipolar Spherical Harmonic (BipoSH) representation. We discuss an effective numerical algorithm, Code for Non-Isotropic Gaussian Sky (CoNIGS) to generate nSI realizations of Gaussian CMB temperature field, specific non-zero BipoSH coefficients. When the SI violation is captured by a specific, or few, bipolar multipoles, L, of BipoSH , the computational costs of making nSI simulation scales $\sim l_{max}^{1.70}$ in our method. Realizations of nSI CMB temperature field are obtained for non-zero quadrupolar ($L = 2$) BipoSH measurements by WMAP, dipolar asymmetry ($L = 1$) with a *scale dependent* modulation field as measured by Planck and also for Doppler boosted CMB temperature field. For a scale independent modulation field, nSI maps can be produced easily by multiplying SI map with a modulation field, but cannot be implemented for a *scale dependent* modulation. Our method, CoNIGS can incorporate any *scale dependent* modulation field in terms BipoSH coefficients, and can produce nSI maps. For SI violation such as Doppler boost that remap the sky, our approach also provides an important advantage of providing maps on the original pixelization, thus avoiding, possible interpolation errors.

1 Introduction

Cosmic Microwave Background (CMB) is a very powerful probe of our Universe. Several important CMB experiments like COBE, WMAP, Planck, BOOMERanG, ACT, SPT etc. have opened an era of precision cosmology. Recent measurements from Planck [1] of the CMB temperature power spectrum matches well with the minimal ΛCDM model at angular scales smaller than 2 degrees. However at large angular scales, Planck [2] has revealed possible signature of Statistical Isotropy (SI)

*suvodip@iucaa.ernet.in
†tarun@iucaa.ernet.in

violation of CMB temperature field, which is beyond our present understanding. SI violation can be measured by Bipolar Spherical Harmonic (BipoSH) coefficients, introduced in CMB temperature measurements by Hajian and Souradeep [3, 4]. These are the linear combinations of off-diagonal terms in the covariance matrix and arise from the correlation between different CMB multipoles l, in Spherical Harmonics (SH) space.

Violation of SI is an inevitable consequence of known effects such as weak lensing, Doppler boost due to our motion with respect to the CMB rest frame [5, 6, 7]. SI violation is also expected from theoretically motivated possiblities such as non-trivial cosmic topology [8]. Presence of systematics in experiments like non-circular beam, masking etc. can also lead to SI violation. Detection of non-SI (nSI) signal that are not consistent with SI Cosmological models, can indicate a breakdown of Cosmological Principle (CP). Recently, WMAP [9] and Planck [2] measured a significant detection of non-zero BipoSH coefficients. A viable solution for WMAP's nonzero measurement of BipoSH is due to non-circularity of WMAP beam as shown by Joshi et al. [10]. However the origin of the BipoSH measurements from Planck are beyond the understanding of present SI Cosmological models. Thus quest for measuring nSI signal are of primary interest in understanding our Cosmological model, and also to remove the effect of systematics on CMB maps.

To investigate these effects, it is important to generate large number of simulations of nSI Gaussian CMB maps of temperature and polarization field. These simulations help in determining the statistical properties of nSI sky due to the physical process mentioned above and the ability of different estimators on sky maps to discern & distinguish between them. Various algorithms are available to incorporate weak lensing of CMB temperature and polarization maps [11, 12, 13, 14]. Non-Gaussian (NG) SI maps were made for studying non-Gaussianity in CMB sky by Liguori et al. [15] and Rocha et al. [16].

In this paper we present an efficient numerical algorithm, Code for Non-Isotropic Gaussian Sky (CoNIGS), to make Monte-Carlo realizations of nSI CMB temperature field. In this algorithm, we efficiently Cholesky decompose the covariance matrix in SH space. A key feature of our approach is that it evades the need for the resampling on locally cartesian grid with subsequent polynomial interpolation as required for Doppler boosted CMB sky, or lensed sky maps.

The paper is organised as follows, in Sec. 2, we review some of the existing topics, we use in this paper. In Sec. 3, we discuss the method to make nSI Gaussian maps of temperature. In Sec. 4, we discuss the results from the simulated maps for three different cases. Discussion and conclusions are given in Sec. 5.

2 Review of statistical properties of CMB temperature field

In our present understanding, temperature fluctuation of CMB originated from the quantum fluctuations of the ground state of the single inflation scalar field. This implies that the statistics of the CMB temperature fluctuation is expected to be Gaussian with zero mean. Recent results from experiments like Planck [17] also place fairly strong constraints on primordial Non-Gaussianity (NG) to be consistent with zero. In the next sections, we briefly review the statistics of CMB temperature field and its covariance matrix.

2.1 CMB temperature field

Temperature anisotropy of CMB sky map $\Delta T(\hat{n})$ can be expanded in the orthonormal space of Spherical Harmonics (SH) functions on the sphere,

$$\Delta T(\hat{n}) = \sum_{lm} a_{lm} Y_{lm}(\hat{n}), \tag{1}$$

where a_{lm} are the coefficients of Gaussian random field in SH space. The statistics of any Gaussian distribution can be specified by its covariance matrix, $G_{ij} \equiv \langle a_i^* a_j \rangle$ where $i = l(l+1) + m - 3$ is a single positive index representing an SH multipole (l, m). The probability distribution of the temperature field is given by,

$$P[a_j] = \frac{1}{(2\pi)^{n/2}\sqrt{|G|}} \exp\left[-(a_i^* G_{ij}^{-1} a_j)\right], \tag{2}$$

where, we assume the Einstein summation rule. Given the largest multipole l_{max}, the covariance matrix is of size

$$N = l_{max}(l_{max}+1) + l_{max} - 3. \tag{3}$$

Under the assumption of SI temperature field, the two point correlation function on the sphere (sky) depends only upon angular separation between the two points. This implies a diagonal the covariance matrix, G, given by the angular power spectrum C_l by,

$$G_{ij} \equiv \langle a_i^* a_j \rangle = C_l \delta_{ij}. \tag{4}$$

But for SI violated maps, covariance matrix is not diagonal. The non-zero off-diagonal elements of Non-SI (nSI) temperature field can be expressed by Bipolar Spherical Harmonic (BipoSH) coefficients introduced by Hajian and Souradeep [3]. In the next section we review the BipoSH coefficients and its connection to the covariance matrix.

2.2 Formalism of BipoSH coefficients for CMB temperature field

As mentioned in the previous section, the CMB temperature fluctuations are Gaussian random field with zero mean and we can express the statistics of this field by the two point correlation function. In the full generality, the two point correlation of SH coefficients of the CMB temperature anisotropy $\langle a_i a_j^* \rangle$ can be expanded in the tensor product basis of two SH space as,

$$\langle a_i^* a_j \rangle = \sum_{LM} A_{ll'}^{LM} (-1)^{m'} C_{lml'-m'}^{LM}, \tag{5}$$

where $A_{ll'}^{LM}$ are called the Bipolar Spherical Harmonics (BipoSH) coefficients [3] and $C_{lml'm'}^{LM}$ are the Clebsch-Gordan (CG) coefficients. These BipoSH coefficients with $L = 0, M = 0$, are the diagonal elements related to the angular power spectrum by, $A_{ll'}^{00}\delta_{ll'} = (-1)^l C_l \sqrt{(2l+1)}$.
For nSI case, BipoSH coefficients are non-zero for $L \neq 0, M \neq 0$. We can relate eq.(5) to the covariance matrix (G) by,

$$\begin{aligned} G_{ij} \equiv \langle a_j^* a_i \rangle &= \sum_{LM} A_{ll'}^{LM} (-1)^{m'} C_{lml'-m'}^{LM}, \\ G_{ij} \equiv \langle a_j^* a_i \rangle &= C_l \delta_{ij} + \sum_{LM;L\neq 0} A_{ll'}^{LM} (-1)^{m'} C_{lml'-m'}^{LM}, \end{aligned} \tag{6}$$

where i and j are related with l, m and l', m' by

$$\begin{aligned} i &= l(l+1) + m - 3, \\ j &= l'(l'+1) + m' - 3. \end{aligned} \tag{7}$$

Using the definition of BipoSH spectra from WMAP [9], eq.(6) becomes,

$$G_{ij} = C_l \delta_{ij} + \sum_{LM;L\neq 0} (-1)^{m'} \alpha_{ll'}^{LM} \frac{\Pi_{ll'}}{\Pi_L} C_{l0l'0}^{L0} C_{lml'-m'}^{LM}. \tag{8}$$

Where, BipoSH coefficients, $A_{ll'}^{LM}$, are related with BipoSH spectra, $\alpha_{ll'}^{LM}$, by

$$A_{ll'}^{LM} = \alpha_{ll'}^{LM} \frac{\Pi_{ll'}}{\Pi_L} C_{l0l'0}^{L0}, \tag{9}$$

and following the notation in [18]

$$\Pi_{l_1 l_2 \ldots l_n} = \sqrt{(2l_1+1)(2l_2+1)\ldots(2l_n+1)}. \tag{10}$$

Any non-zero measurement of BipoSH coefficients indicates violation of SI of our Universe. Weak lensing, Doppler boost, masking and non-circular beam are some of important effects that leads to SI violation in the observed CMB sky even when the underlying CMB signal is SI.

3 Method: Simulations of nSI CMB temperature field

The central difference between the covariance matrix in SH space for SI and nSI CMB map is the presence of off-diagonal terms in the SH space covariance matrix. This implies that different modes of CMB, (l, m), are not independent in SH space in case of nSI maps. The key idea we implement is to make a change of basis from SH space to another space in which this covariance matrix is diagonal. A linear transformation does not change the Gaussian statistics of the field. In the new space the different modes are no more correlated but realization of CMB temperature in this basis are manifestly SI violated. On performing an inverse transformation of CMB temperature map from the new space to SH space, gives us the nSI CMB temperature maps in SH space.

3.1 Cholesky decomposition of the covariance matrix

In this section, we discuss the method of diagonalization of the covariance matrix by Cholesky Decomposition (CD) algorithm. In CMB analysis, CD has been implemented by Gorski [19] for diagonalization of coupling matrix for the spherical harmonic on the cut sky. When SI violation is captured in a limited set of non-zero BipoSH coefficients, it is possible to implement an efficient code that scale $N^{0.853}$ implying $\sim l_{max}^{1.70}$ (l_{max} determines the angular resolution of the map), instead of the well known $N^3/6$ scaling of the CD algorithm in general cases. The covariance matrix, G, of a Gaussian distribution is always positive definite which satisfies the following two conditions [20],

1. For any vector $y \in \mathbb{R}, y^T G y > 0$. This condition implies a strong constrain on diagonal terms, i.e. $G_{ii} > 0$.

2. The determinant of the covariance matrix should be positive. i.e. $|G| \geq 0$. Since the inverse of the covariance matrix, (G^{-1}) must exist, this makes $|G| > 0$.

Also because of the dependence of the elements of covariance matrix on CG coefficients as mentioned in eq.(8), the elements of covariance matrix also obey the properties of CG coefficients [18],

$$\begin{aligned} C^{LM}_{lml'm'} &\neq 0; \qquad \text{iff } |l_1 - l_2| < L < l + l';\ m + m' = M; \\ C^{L0}_{l_1 0 l_2 0} &\neq 0; \qquad \text{iff } l_1 + l_2 + L = 2n;\ \text{n is an integer;} \end{aligned} \tag{11}$$

Due to the conditions mentioned in eq.(11), the covariance matrix is sparsely populated, which reduces the number of loops. This makes it possible to efficiently diagonalise the covariance matrix. Cholesky decomposition leads to decomposition of covariance matrix into a lower triangular matrix L and its transpose L^t,

$$G = LL^t, \tag{12}$$

where elements of L are related to the elements of G by [20],

$$\begin{aligned} L_{ii} &= \sqrt{(G_{ii} - \sum_{k=1}^{i-1} L_{ik}^2)}, \\ L_{ji} &= \frac{(G_{ij} - \sum_{k=1}^{i-1} L_{ik} L_{jk})}{L_{ii}}; \qquad j = i+1, ...n. \end{aligned} \tag{13}$$

On performing CD on covariance matrix (G), the modification to the probability distribution function eq.(2) is,

$$\begin{aligned} P[a_j] =& \frac{1}{(2\pi)^{n/2}\sqrt{|G|}} \exp\left[-(a_i^*(LL^t)^{-1}_{ij} a_j)\right], \\ =& \frac{1}{(2\pi)^{n/2}\sqrt{|G|}} \exp\left[-(a_i^*(L^t)^{-1} L^{-1} a_j)\right], \\ =& \frac{1}{(2\pi)^{n/2}\sqrt{|G|}} \exp\left[-(L^{-1}a_i^*)^t (L^{-1} a_j)\right], \\ =& \frac{1}{(2\pi)^{n/2}\sqrt{|G|}} \exp\left[-x^t I x\right], \end{aligned} \tag{14}$$

where, we have defined $x_j = L^{-1}_{ji} a_i$. x is the array of CMB temperature map in the new space, where the variance of every element x_i is Gaussian distributed with unit variance. On performing inverse of this transformation, we get, $a_i = L_{ij} x_j$. This map a_i, is manifestly SI violated and averages over random realizations of a_i would match the input BipoSH coefficients.

3.2 Algorithm for generating nSI CMB temperature realizations

In the previous section we discussed the key idea of making nSI simulations of CMB temperature field. In this section we discuss the logical steps we use to produce these nSI maps.
To efficiently diagonalize the covariance matrix of size $N \approx l^2_{max}$, we use the properties of CG coefficients mentioned in eq.(11). For a given value of angular power spectra C_l and BipoSH spectra $\alpha^{LM}_{ll'}$, we develop a numerical code to diagonalize the covariance matrix G, into lower triangular matrices L and L^t. In Fig. 1, we plot the computational time required for the diagonalization of the covariance matrix. By using the properties of CG coefficients, CoNIGS, scales with size of the matrix, N by $N^{0.853}$ implying $\sim l^{1.70}_{max}$. For a given angular power spectra C_l and BipoSH power spectra $\alpha^{LM}_{ll'}$, we need to generate the lower triangular matrix L, only once, and different

realizations can be obtained by multiplying L with Gaussian realizations, x_i, of unit variance with different seed value. The temperature realizations a_i, in SH space are complex numbers with both real and imaginary part, i.e.

$$a_i = c_i + i\, d_i, \tag{15}$$

where, c_i and d_i are the real Gaussian random variables. But for the azimuthal symmetric modes ($m = 0$), imaginary part d_i vanishes. Hence, the maps, x_i in the new basis should be transformed both to the real part c_i and imaginary part d_i of the temperature maps a_i. We define x_i^R and x_i^I, as two parts of the maps x_i, which contribute respectively to the real and imaginary part of the maps a_i, in SH space. Then the variance of x_i should satisfy,

$$\begin{aligned} &\sigma^2_{x^R} + \sigma^2_{x^I} = \sigma^2_x = 1; && \text{for } m \neq 0 \text{ modes} \\ &\sigma^2_{x^R} \equiv \sigma^2_x = 1; && \text{for } m = 0 \text{ modes.} \end{aligned} \tag{16}$$

This is a very important step to produce realizations that obeys the same statistics. Following are the steps incorporated to produce the nSI realizations of CMB temperature field using CoNIGS.

1. Implement CD on the covariance matrix G, to produce lower triangular matrices, L and L^t.
2. Generate Gausssian random variables x_i^R and x_i^I with variance satisfying eq.(16). This is the temperature map, x_i, in the new space.
3. Multiply x_i with the lower triangular matrix L, to obtain temperature map, a_i in SH space.
4. Using the alm2map package in HEALPix [21], generate the maps.

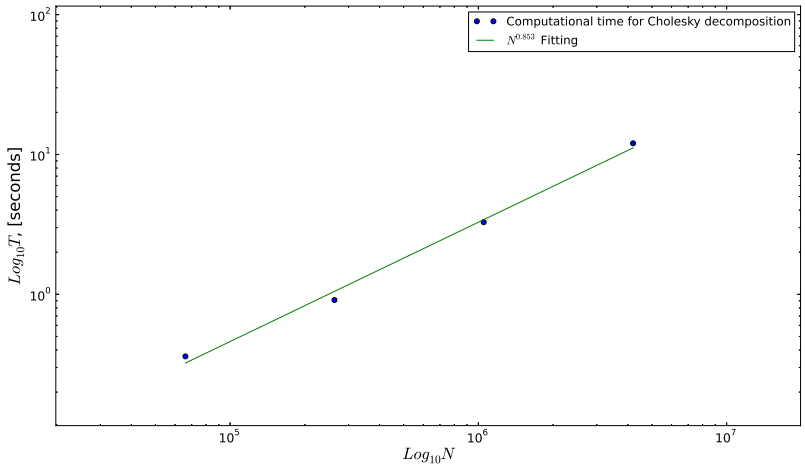

Figure 1: Scaling of computational time with the dimension of the SH space covariance matrix, N. N depends upon l_{max} by $N \approx l^2_{max}$. Blue circles are the time taken by the code for different values of l_{max}. For $l_{max} = 2048$, computational time on a single processor of 2.60 GHz is $\sim$ 12 seconds. Green line is fitted to these circles with $N^{0.853} \sim l^{1.70}_{max}$.

4 nSI realizations of CMB temperature field

We study three different cases of nSI maps, with the BipoSH spectra that have come under discussions and study due to results obtained by recent experiments like WMAP and Planck.

1. The quadrupolar ($L = 2$) BipoSH spectra as measured by WMAP [9].

2. BipoSH spectra for $L = 1$ with a *scale dependent* modulation strength which results in dipolar asymmetry as measured by Planck [2].

3. The Doppler boosted CMB temperature map with non-zero BipoSH spectra for $L = 1$ by Planck [6].

4.1 Quadrupolar asymmetry: WMAP 7 year measurement of non-zero BipoSH spectra $L = 2$.

The measurement of BipoSH spectra for $L = 2, M = 0$ by WMAP [9] is a signature of SI violation. With angular power spectrum C_l and only non-zero BipoSH spectra, α^{20}_{ll} and α^{20}_{ll+2}, we obtain the covariance matrix, G using eq.(8). By using the numerical algorithm CoNIGS, we obtain the nSI realization of CMB temperature field for $l_{max} = 2048$, given in Fig. 2. To show the visual effect of the non-zero BipoSH coefficients, we take the difference of nSI realization with SI realization for the same seed value and is plotted in Fig. 3. The range of the variation of difference in temperature fluctuation is $[-5.56\mu\text{K}, 5.74\mu\text{K}]$, which is $\sim$ 100 times smaller than the range of temperature fluctuation of SI map.
The average two-point correlation function estimated from a Monte Carlo ensemble these maps should match the input covariance matrix, G. To test the consistency of the two point correlation for these nSI maps with the input covariance matrix, we obtain 1000 realizations of nSI maps, and then using a BipoSH estimation code [22] we obtain the two point correlations from the simulated temperature maps. The comparison between input and output values of angular power spectra and BipoSH spectra are plotted in Fig. 4 and Fig. 5 respectively. The comparison between input and output power spectra of temperature field ensures that the ensemble averages of nSI realizations generated by our method recover the input angular power spectra and BipoSH spectra. This provides an efficient means for creating Monte Carlo ensembles of CMB maps useful in studying different models of SI violation and to study their statistical properties.

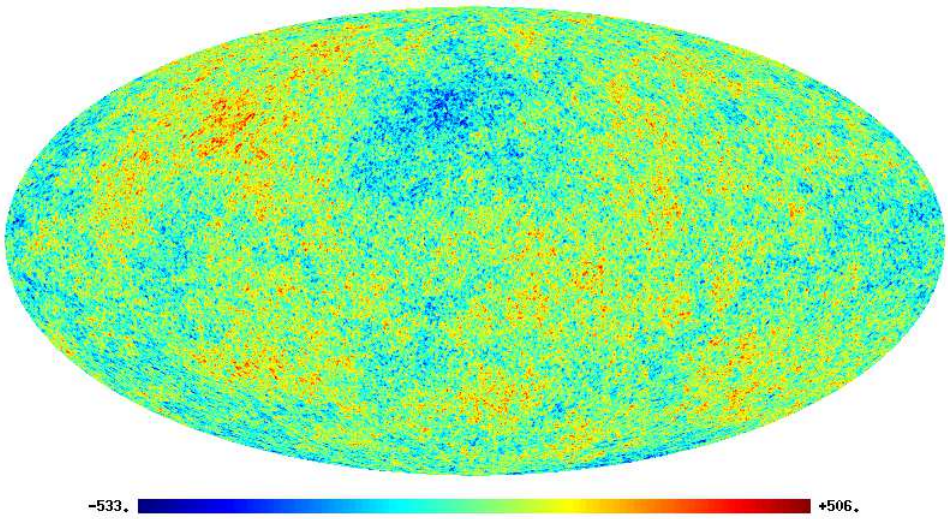

Figure 2: nSI realization for CMB temperature field with $L = 2$ Bipolar spectra produced using CoNIGS.

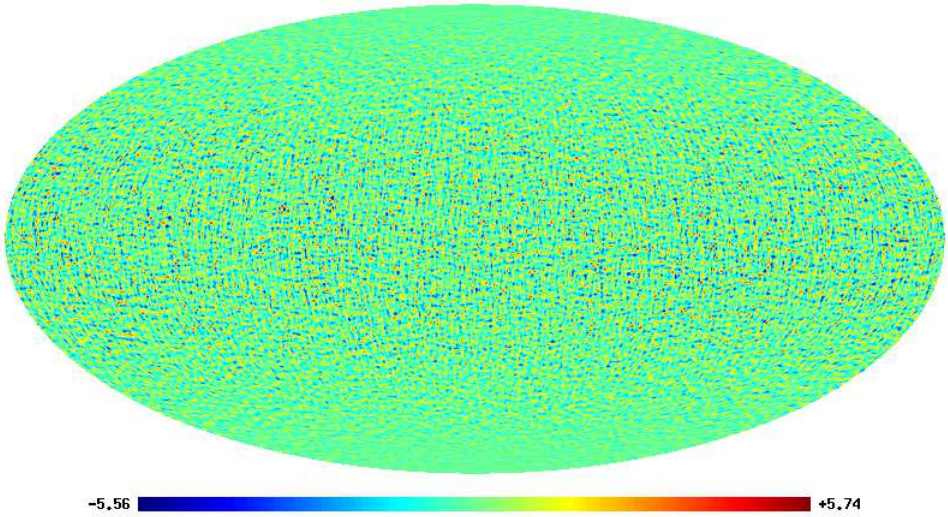

Figure 3: Difference between the nSI map with $L = 2$ non-zero BipoSH spectra and SI map for the same seed of random realization. The difference in temperature is in the range $[-5.56\mu K, 5.74\mu K]$ to be compared to the range of $[-534\mu K, 505\mu K]$ of nSI map in Fig. 2.

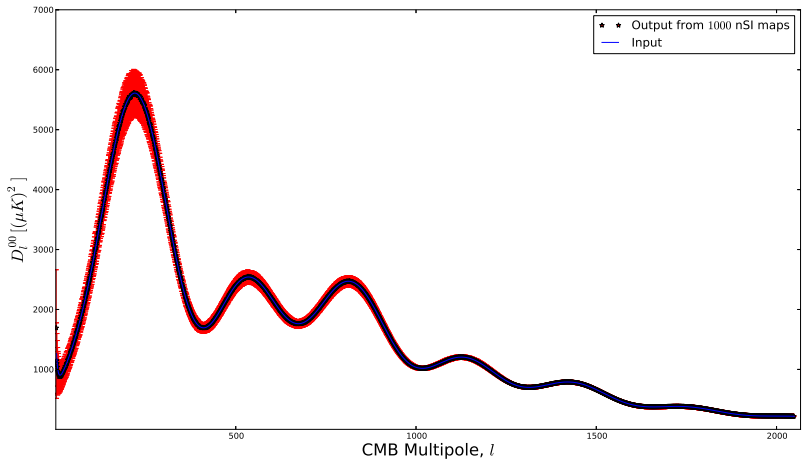

Figure 4: Comparison of input and output values of $D_l^{00} = l(l+1)C_l/2\pi$ obtained from 1000 Non-SI maps

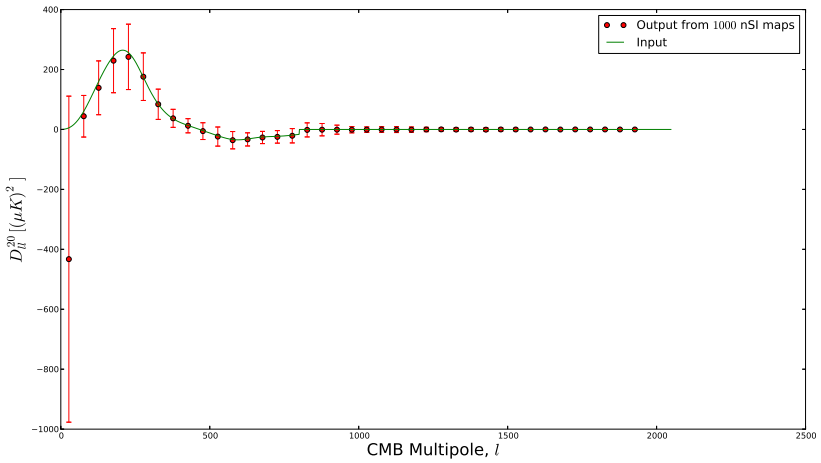

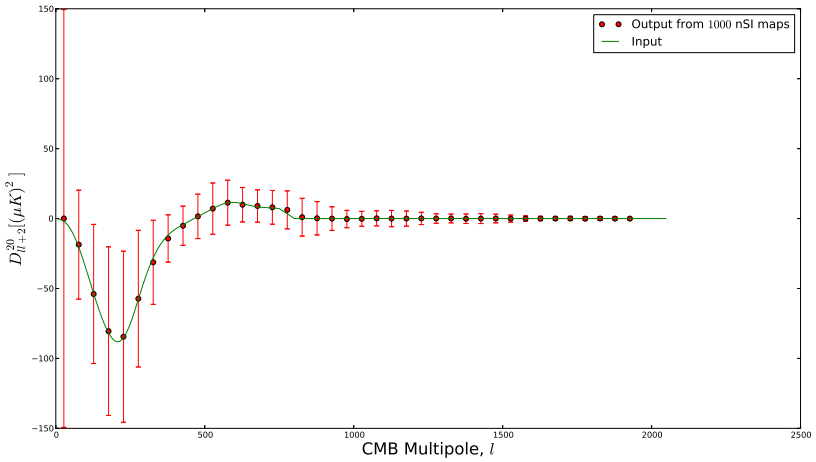

Figure 5: Comparison of BipoSH spectra, $D_{ll}^{20} = l(l+1)\alpha_{ll}^{20}/2\pi$ (top) and $D_{ll+2}^{20} = l(l+1)\alpha_{ll+2}^{20}/2\pi$ (bottom) obtained from 1000 realizations with the input value of D_{ll}^{20} and D_{ll+2}^{20}. Here the BipoSH spectra are binned with $\Delta l = 50$.

4.2 Dipolar asymmetry: Scale dependent non-zero dipolar ($L = 1$) BipoSH spectra from Planck measurement.

The nSI estimator on Planck CMB map, measured a 3.7σ detection of BipoSH spectra for $L = 1$, modeled as a dipolar modulation of SI CMB, with a *scale dependent* modulation strength [2]. Presence of modulation leads to nSI CMB temperature field. Making such nSI realizations for a scale independent modulation strength can easily be obtained by multiplying an SI realization with a given scale independent modulation function. However, this procedure cannot be used to make nSI realization for a *scale dependent* modulation strength. CoNIGS, is an efficient method to produce nSI realization for a *scale dependent* modulation strength. In CoNIGS, we encapsulate *scale dependent* modulation in terms of BipoSH coefficients, which are the complete representation for any SI violation. In terms of BipoSH spectra, *scale dependent* modulation strength can be incorporated by the expression,

$$\alpha^{10}_{ll+1} = m^1_l \left[C^{TT}_l + C^{TT}_{l+1} \right] \frac{\Pi_{ll+1}}{\sqrt{4\pi}\Pi_1} C^{10}_{l\,0\,l+1\,0}, \tag{17}$$

In our method of producing nSI realizations, we can easily incorporate the *scale dependent* modulation strength in terms of the $L = 1$ BipoSH coefficients, and for any arbitrary choice of modulation function, our numerical code, CoNIGS can produce the corresponding nSI realizations.

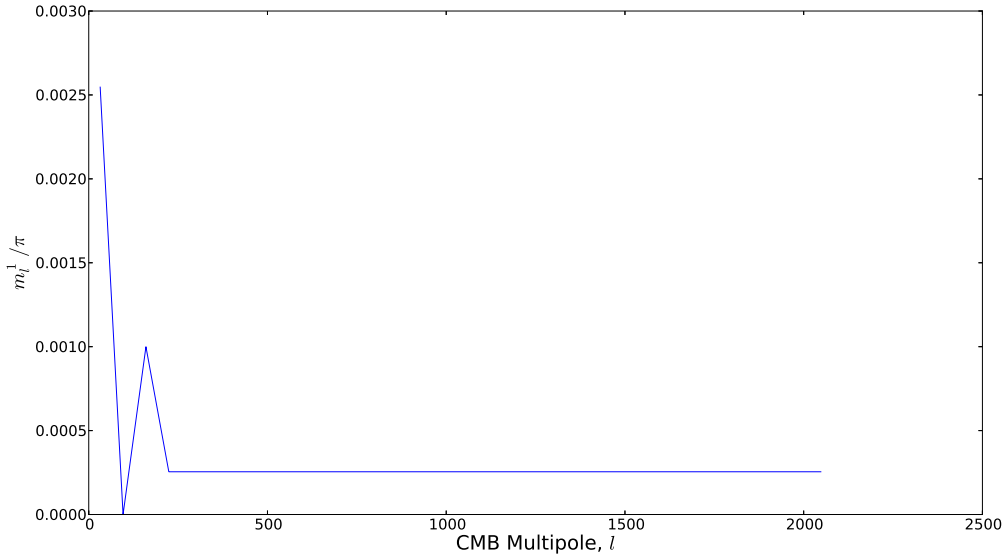

Figure 6: Modulation strength, m^1_l, with a scale dependence, used for producing nSI maps. Similar result is measured by Planck [2].

Using CoNIGS we make realizations of such nSI CMB sky with the BipoSH spectra for $L = 1$, with a *scale dependent* modulation field, m^1_l, given in Fig. 6. This complicated modulation strength is taken to imitate the modulation strength as measured by Planck [2]. In Fig. 7, we plot an nSI realization and the corresponding difference between nSI realization and SI realization for the same random realization is plotted in Fig. 8. Whereas, for a fixed value of $m_1 = 0.008$, we generated the nSI realizations. The difference between the nSI map (with fixed $m_1 = 0.008$) and the corresponding SI map is plotted in Fig. 9. Fixed modulation strength results in fluctuation at all scales in the

difference map given in Fig. 9, in contrast, *scale dependent* modulation leads to more fluctuation at large angular scale as can be seen in Fig. 8. Again to test the consistency of nSI maps with the input statistics, we obtain two-point correlation of 1000 nSI realizations using a BipoSH estimation code [22] and then compare the angular power spectrum and BipoSH spectra with the given input value of BipoSH spectra. The comparison between input and output values of BipoSH spectra are plotted in Fig. 10.

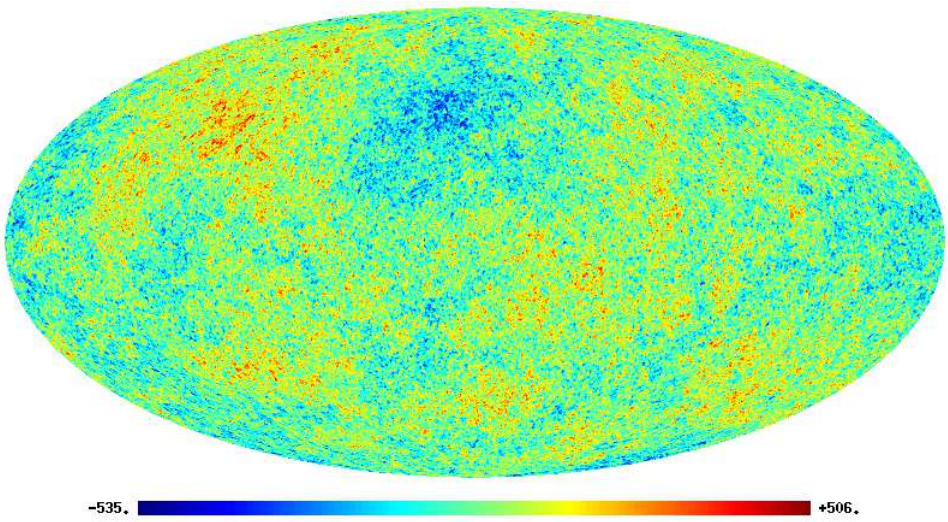

Figure 7: nSI map produced using CoNIGS with $L = 1$ non-zero BipoSH spectra due to dipolar asymmetry with a *scale dependent* modulation strength given in Fig. 6 as measured by Planck [2].

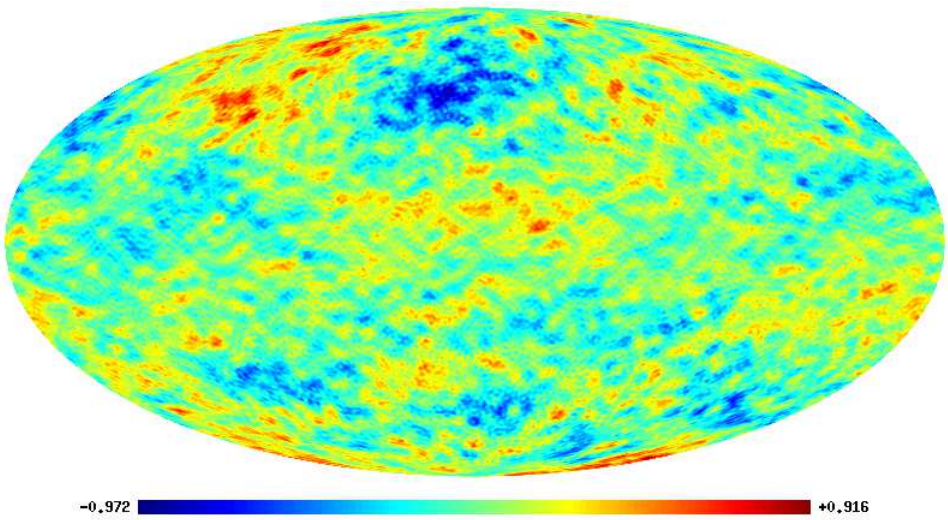

Figure 8: Difference between the SI and nSI realization with $L = 1$ BipoSH spectra for *scale dependent* modulation strength given in Fig. 6. The difference in temperature is in the range $[-0.972\mu K, 0.916\mu K]$ about ~ 500 times smaller than nSI map given in Fig. 7.

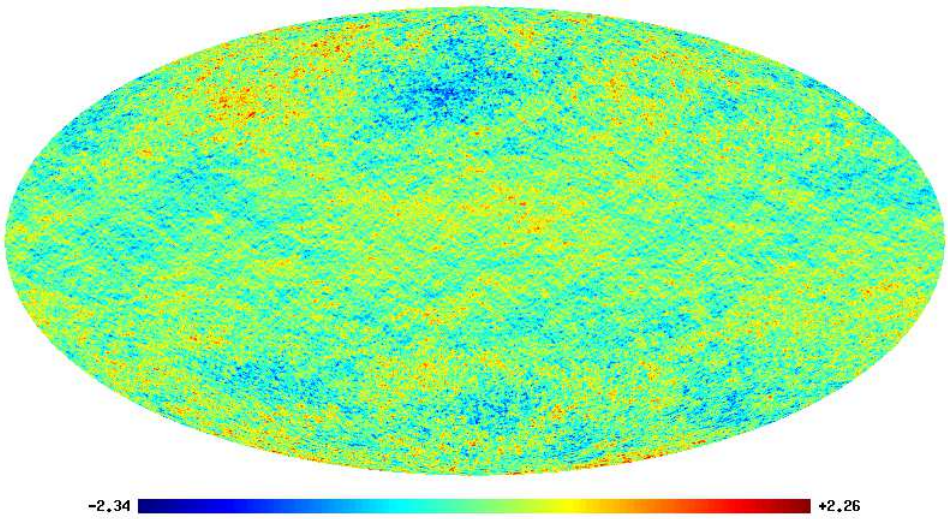

Figure 9: Difference between the SI and nSI realization with $L = 1$ BipoSH spectra for fixed modulation strength, $m_1 = 0.008$. The difference in temperature is in the range $[-2.34\mu K, 2.26\mu K]$ about ~ 250 times smaller than nSI map.

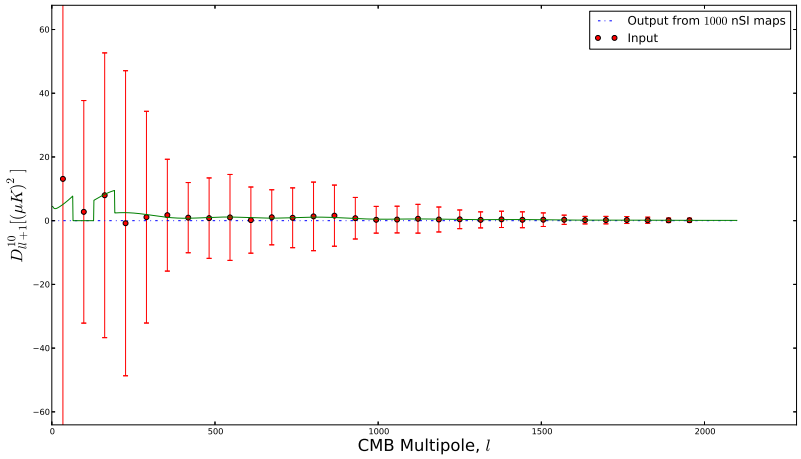

Figure 10: Comparison of BipoSH spectra, $D^{10}_{ll+1} = l(l+1)\alpha^{10}_{ll+1}/2\pi$ obtained from dipolar asymmetric 1000 realizations of CMB temperature sky with the input value of D^{10}_{ll+1} for a *scale dependent* modulation, m^1_l given by Fig. 6. Here the BipoSH spectra are binned with $\Delta l = 64$. The error bar for the 1st bin is 168. The blue line plots zero BipoSH spectra. Using minimum variance estimator [23, 24], a significant detection of BipoSH spectra is made by Planck [2].

4.3 Doppler boost: Non zero dipolar ($L = 1$) BipoSH spectra from our local motion.

Doppler boost of CMB temperature & polarization field due to our local motion, with velocity ($\beta \equiv |v|/c = 1.23 \times 10^{-3}$) induces non-zero dipolar ($L = 1$) BipoSH coefficients as shown by Mukherjee et al. [7]. Recent result from Planck [6] estimated β from the off-diagonal terms of the

SH space covariance matrix which are related to the $L = 1$ BipoSH coefficients. Doppler boosting of CMB temperature field results into two kinds of effects, modulation and aberration. An important merit of our method for this case, is that it avoids errors arising out of the resampling on locally cartesian grids with subsequent polynomial interpolation that could be envisaged along the lines of algorithm used to produce weak lensed CMB maps by Lewis [11]. The linear order effect of Doppler boost on CMB temperature field leads to non-zero BipoSH spectra given by [6, 7]

$$\alpha^{10}_{ll+1} = \beta\left[(l+b_\nu)C^{TT}_l - (l+2-b_\nu)C^{TT}_{l+1}\right]\frac{\Pi_{ll+1}}{\sqrt{4\pi}\Pi_1}C^{10}_{l\,0\,l+1\,0}, \tag{18}$$

where, b_ν is the frequency dependent effect on Doppler boost given by [6],

$$b_\nu = \frac{\nu}{\nu_0}\coth\left(\frac{\nu}{2\nu_0}\right) - 1, \tag{19}$$

with $\nu_0 = 57$ GHz. We estimate the BipoSH spectra with $b_\nu \approx 3$ corresponding to $\nu = 217$ GHz. We make nSI realization of CMB temperature sky Fig. 11 with induced Doppler boost for the value of $\beta = 1.23 \times 10^{-3}$. The difference between nSI map and the corresponding SI map for the same seed is plotted in Fig. 12. The realizations produced by CoNIGS are manifestly nSI and have non-zero value of BipoSH spectra for $L = 1$, which we recover back from a BipoSH estimation code [22]. In Fig. 13, we compare the consistency of input BipoSH spectra with the BipoSH spectra from 1000 realizations.

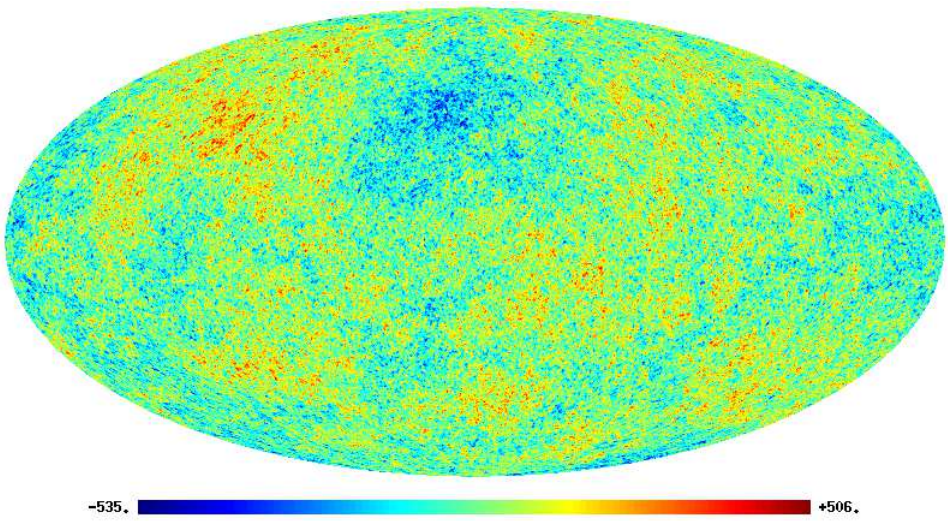

Figure 11: nSI map produced using CoNIGS with $L = 1$ non-zero BipoSH spectra due to Doppler boost for $\beta = 1.23 \times 10^{-3}$.

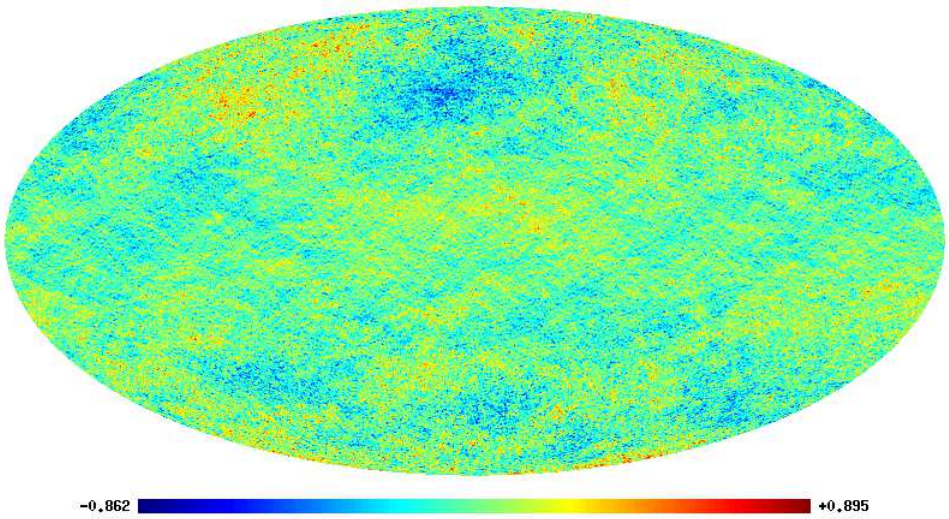

Figure 12: Difference between the SI map and nSI map produced with $L = 1$ BipoSH spectra. The difference in temperature is in the range $[-0.862\mu K, 0.895\mu K]$ which is ~ 500 times smaller than range of flucutuation in the corresponding nSI map given in Fig. 11.

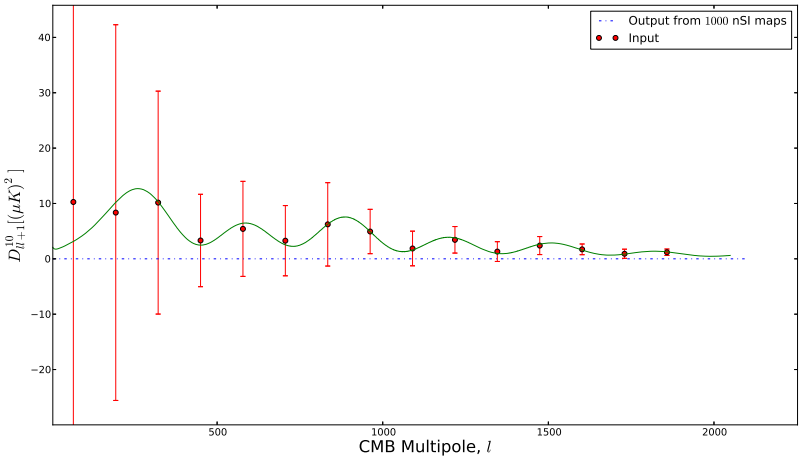

Figure 13: Comparison of BipoSH spectra, $D^{10}_{ll+1} = l(l+1)\alpha^{10}_{ll+1}/2\pi$ obtained from Doppler boosted 1000 realizations of CMB temperature sky with the input value of D^{10}_{ll+1}. Here the BipoSH spectra are binned with $\Delta l = 128$. The error bar for the 1st bin is 160. The blue line plots zero BipoSH spectra. The deviation in Doppler boosted BipoSH spectra from the blue line indicates the possibility for detection of β from the small angular scales of CMB temperature field. Using quadratic estimators a significant detection of β is made by Planck [6].

5 Conclusion

Statistical Isotropy (SI) violation of CMB temperature and polarization maps are an unavoidable consequence of weak lensing by large scale structures, Doppler boost due to moving observer's frame. Many observational systematics like masking, non-circularity of beam etc. can also leads

to SI violation of CMB temperature field. Recent experiments like WMAP and Planck measured statistically significant non-zero BipoSH coefficients. A likely explanation of non-zero quadrupolar ($L = 2$) BipoSH detection by WMAP as arising from uncorrected non-circular beam effect is given by Joshi et al. [10]. Doppler boost due to our local motion leads to $L = 1$ BipoSH spectra, which are measured by Planck [6]. Planck also made a 3.7σ detection of BipoSH spectra for $L = 1$, called the dipolar asymmetry [2], which is beyond the understanding of present SI Cosmological models. This measurement indicates, CMB temperature field to be manifestly SI violated. To study these effects and to understand the statistics of Non-SI (nSI) CMB sky, it is important to make nSI realizations of CMB temperature & polarization field.

In this paper, we have developed an efficient method, Code for Non-Isotropic Gaussian Sky (CoNIGS) for generating nSI Gaussian realizations of CMB temperature field. nSI CMB temperature field leads to non-zero off-diagonal (BipoSH coefficients) terms in the SH space covariance matrix, in contrast to the SI temperature field that has only non-zero diagonal (angular power spectra) terms. The central idea of the technique is to diagonalise the covariance matrix using Cholesky Decomposition (CD) mentioned in eq.(12). Also the dependence of elements of covariance matrix on Clebsch-Gordan (CG) coefficients as mentioned in eq.(8), ensures that the covariance matrix is sparsely populated. So, we can diagonalise the matrix faster than the usual CD. The time taken for diagonalization using CoNIGS depends on the dimension of matrix, N by $N^{0.853}$ implying a $\sim l_{max}^{1.70}$ as given in Fig. 1, in contrast to the usual CD, which depends upon N by $N^3/6$.

Using this method we generated nSI realizations for temperature field with BipoSH spectra as measured by WMAP for $L = 2$, given in Fig. 2. The difference between the SI and nSI map of the same random realization are plotted in Fig. 3. The comparison of angular power spectra and BipoSH power spectra from 1000 simulations with the input angular power spectra and BipoSH power spectra are plotted in Fig. 4 and Fig. 5 respectively. Planck measurement [2] of BipoSH coefficients for $L = 1$, dipolar asymmetry, shows a *scale dependent* modulation. For modulation with no scale dependence, nSI map can easily be produced by multiplying modulation function with the SI map, but cannot be implemented for *scale dependent* modulation. By incorporating SI violation in terms of BipoSH coefficients, we can make nSI realizations for any *scale dependent* modulation field. Our method, CoNIGS, is the only efficient method to produce nSI realizations of CMB temperature field for a *scale dependent* modulation field, m_l^1 given in Fig. 6, similar to the measurement by Planck [2]. Corresponding nSI maps and the difference between the SI and nSI map for the same random realization are plotted in Fig. 7 and Fig. 8 respectively. In Fig. 9, we plotted the difference map between SI realization and nSI realization with a scale independent modulation field value, $m_1 = 0.008$. Fig. 8 and Fig 9 shows the effect of a *scale dependent* and scale independent modulation field respectively on an SI CMB temperature field. The presence of prominent fluctuations in the difference map, Fig. 8, at large angular scales and absence of fluctuations at small angular scales are the signature of *scale dependent* modulation field given in Fig. 6, whereas, for constant modulation field fluctuations are present at all angular scales as given in Fig. 9. The comparison between the input angular power spectra with the output angular power spectra is plotted in Fig. 4. The plot for comparison between BipoSH power spectra from 1000 simulations with the input BipoSH power spectra is given in Fig. 10. We also made the realizations of Doppler boosted CMB temperature maps which gives rise to $L = 1$ BipoSH spectra. In this process we can easily include the aberration effect evading the need for resampling on locally cartesian grid with subsequent polynomial interpolation for pixelization, necessary in methods employed in generating weak lensed CMB map. The realization for nSI temperature sky and the difference between nSI and SI realization are given in Fig. 11 and Fig. 12 respectively. The comparison of the angular power spectra and BipoSH spectra from 1000 simulations with the input angular power spectra and BipoSH spectra are plotted in Fig. 4 and Fig. 13 respectively. CoNIGS is a fast and efficient

method for producing nSI realizations of CMB temperature field. This is readily extendable to CMB polarization maps. This is a very important tool to understand the statistics and also to estimate any signal in the nSI temperature field. This method can also be extended to make lensed CMB maps by the covariance matrix for a given lensing potential.

Acknowledgement:
We have used the HPC facility at IUCAA. We also used the HEALPix [21] package to make the maps. SM acknowledges Council for Science and Industrial Research (CSIR), India, for the financial support as Senior Research Fellow. SM also thanks Santanu Das and Aditya Rotti for many useful discussions. TS acknowledges support from Swarnajayanti fellowship, DST, India.

References

[1] P. A. R. Ade et al., Planck 2013 results. XV. CMB power spectra and likelihood, preprint arXiv:1303.5075, (2013).

[2] P. A. R. Ade et al. Planck 2013 results. XXIII. Isotropy and Statistics of the CMB., preprint arXiv:1303.5083, (2013).

[3] A. Hajian and T. Souradeep, Astrophys. J. 597, L5, (2003).

[4] T. Souradeep A. Hajian and S. Basak, New Astron.Rev. 50, 889, (2006).

[5] A. Challinor and F. V. Leeuwen, Phys.Rev. D65 103001, (2002).

[6] N. Aghanim et al. Planck 2013 results. XXVII. Doppler boosting of the CMB: Eppur si muove, preprint arXiv:1303.5087, (2013).

[7] S. Mukherjee, A. De and T. Souradeep, preprint arXiv:1309.3800, (2013) .

[8] A. Hajian and T. Souradeep Astro.ph., 1590H (2003).

[9] C. L. Bennett et al.Astrophys.J.Suppl. 192, 17, (2011).

[10] N. Joshi et al., preprint arXiv:1210.7318v2, (2012).

[11] A. Lewis, Phys.Rev. D71, 083008, (2005).

[12] C. M. Hirata et al., Phys.Rev. D 70, 103501, (2004).

[13] S. Das and P. Bode, Astrophys. J. 682, 1, (2008).

[14] S. Basak, S. Prunet and K. Benabed, preprint arXiv:0811.1677, (2008).

[15] M. Liguori, S. Matarrese and L. Moscardini, The Astrophysical Journal 597, 57, (2003).

[16] G. Rocha et al. Mon.Not.Roy.Astron.Soc. 357, 1285, (2005).

[17] P. A. R. Ade et al. Planck 2013 results. XXIV. Constraints on primordial non-Gaussianity, preprint arXiv:1303.5084v1, (2013).

[18] D. A. Varshalovich A. N. Moskalev and V. K. Khersonskii, Quantum Theory of Angular Momentum, World Scientific, (1989).

[19] K. M. Gorski, Astrophys.J. 430, L85, (1994).

[20] G. H. Golub and C. F. V. Loan, Matrix Computations, Johns Hopkins Studies in Mathematical Sciences Press, (1996).

[21] K. M. Gorski et al. ApJ 622, 759, (2005).

[22] N. Joshi, A. Rotti and T. Souradeep, PhysRevD.85.043004, (2012).

[23] W. Hu and T. Okamoto, Astrophys.J., 574, 566, (2002).

[24] D. Hanson, G. Rocha and K. M. Gorski, Mon.Not.Roy.Astron.Soc., 400, 2169, (2009).